IEEE Access
Multidisciplinary | Rapid Review | Open Access Journal

Received September 23, 2020, accepted October 18, 2020, date of publication October 28, 2020,
date of current version November 12, 2020.

Digital Object Identifier 10.1109/ACCESS.2020.3034334

A Low Flicker TRIAC Dimmable Direct AC LED Driver for Always-on LED Arrays

SEONG JIN YUN, (Member, IEEE), YONG KI YUN, (Graduate Student Member, IEEE), AND YONG SIN KIM, (Senior Member, IEEE)
School of Electronic Engineering, Korea University, Seoul 02841, South Korea

Corresponding author: Yong Sin Kim (shonkim@korea.ac.kr)

This work was supported in part by the LG Innotek, and in part by the Basic Science Research Program through the National Research Foundation of Korea (NRF), Ministry of Education, under Grant NRF-2016R1D1A1B04935233.

ABSTRACT Direct AC LED drivers have advantages over conventional LED drivers in size and cost because of no need for bulky and expensive inductive components. However, none of conventional direct AC LED drivers researched so far support triode AC switch (TRIAC) compatibility at low percent flicker. This paper achieves both TRIAC dimmer compatibility and low percent flicker by correlating a phase-cut ratio to luminance and using always-on multi-arrays, respectively, without the need of a dedicated IC. The proposed LED driver consists of a phase-cut/DC converter, a switch controller, a current regulator, and three LED arrays. The experimental results based on commercial 15W LEDs show that the percent flicker of 18.6% @ 120 Hz is achieved with an efficiency of 84.7% and a power factor of 97.3% @ 120 V.

INDEX TERMS Direct AC, LED, percent flicker, TRIAC, dimmable, inductor-less.

I. INTRODUCTION

For indoor household and commercial lighting, light emitting diodes (LEDs) are widely replacing incandescent and fluorescent lamps because of their long lifetime and high luminous efficiency [1]–[5]. In conventional lighting systems without using LEDs, triode AC switch (TRIAC) dimmers are used for controlling luminance of resistive loads such as incandescent or halogen light bulbs. However, LEDs without proper control circuits cannot be directly compatible with these TRIAC dimmers because LED drivers may cause visible flicker [6]. Flicker is defined as a change in intensity of a light source caused by the fluctuations of the light source itself, power-line flicker, or incompatibility with an external dimmer. As shown in Fig. 1, flicker can be quantified as two different parameters: percent flicker and flicker index. The percent flicker is the ratio between the maximum light and the minimum light in a cycle. Flicker index, on the other hand, requires the accurate measurement of waveform shape with complex integral math. So the percent flicker is more generally used than the flicker index to qualify the amount of flicker. IEEE PAR1789 standard working group introduces possible health risks of higher percent flicker [7], [8].

The associate editor coordinating the review of this manuscript and approving it for publication was Tariq Masood.

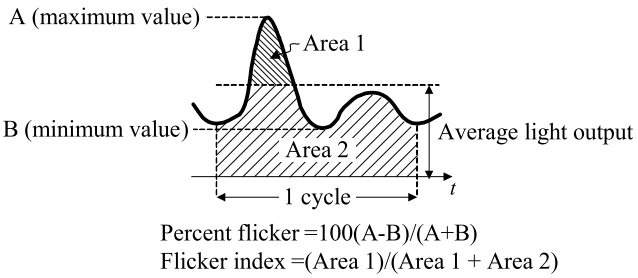

FIGURE 1. The definition of percent flicker and flicker index [7].

Many circuit topologies for a TRIAC dimmable LED driver are based on a switched-mode power supply (SMPS) with a phase angle to current converter that leads to lower flicker [3]. Conventional two-stage topologies in [9]–[13] can achieve aforementioned performances at the expense of many inductive components, large form factor, and high manufacturing costs. The single-stage topologies with power factor correction (PFC) flyback converters are developed to alleviate those problems in two-stage topologies, but still bulky inductive components and large smoothing capacitors with a high voltage rate cannot be avoided [14]–[24].

Recently, direct AC LED driver topologies are developed to reduce form factor and cost compared with conventional SMPS based topologies by directly connecting multiple LED

strings to the rectified AC input without using bulky inductive components [28]–[34]. In order to increase power factor and efficiency, direct AC LED drivers in [28]–[30] adopted either a micro-controller or a dedicated IC for string controls. In [31], a direct AC LED driver using a simple LED bridge structure is introduced without using either a micro-controller or a dedicated IC, but it requires an inductive component for sensing LED sting current. Other direct AC LED drivers in [32], [33] have developed by adding standard operational amplifiers and switches without the need of a dedicated IC, a micro-controller, or an inductive component. However, aforementioned direct AC LED drivers have a significant drawback that yields the percent flicker of 100%. To enhance percent flicker, a direct AC LED driver in [34] adopts a valley fill circuit and achieves the percent flicker of 28%. Nonetheless, both power factor and output power are too low to be used for residential and commercial lighting systems. Furthermore, none of the conventional direct AC LED drivers is TRIAC dimmable.

In this paper, TRIAC dimmable direct AC LED driver with percent flicker less than 20% is proposed. For reducing percent flicker, the proposed LED driver sequentially drives always-on multiple LED strings. Additionally, high power factor, efficiency, and output power are achieved without using a dedicated IC, a micro-controller, or an inductive component. This paper consists as follows: The topologies of conventional LED driver are described in Section II. Section III introduces the basic theory and the circuit implementation of the proposed LED driver. The simulation result and experimental results the proposed LED driver are presented in Sections IV and V, respectively, and followed by conclusion in Section VI.

II. CONVENTIONAL LED DRIVERS

Fig. 2 shows a basic configuration of a TRIAC dimmable LED lighting system. A phase-cut ac voltage v_{IN} is generated by the TRIAC dimmer from an AC line voltage v_{AC} and fed to the TRIAC dimmable LED driver that chops up the voltage waveform by phase angle of θ depending on dimming level. The brightness of the LED array varies in accordance with the output current.

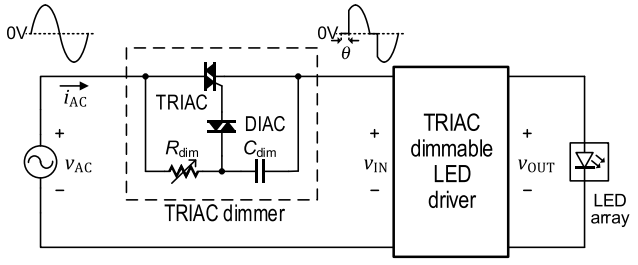

FIGURE 2. Basic configuration of a TRIAC dimmable LED lighting system.

For driving LEDs from AC power supplies, one of the basic approaches is a single-stage AC/DC conversion topology that consists of a full-bridge rectifier (FBR) and a DC/DC converter as shown in Fig. 3(a). Because a single-stage AC/DC converter has wide input voltage range, a flyback converter with a bulky transformer is widely adopted at the expense of large amount of switching and snubber losses [35]. It is suggested that residential and commercial LED lighting sources below 25 W have a minimum power factor of 0.9 [36], but a single-stage AC/DC converter hardly meets this condition. A two-stage AC/DC converter structure in Fig. 3(b) has been developed to reduce those losses and to increase power factor by having an additional power factor correction (PFC) stage for higher cost and larger form factor [37].

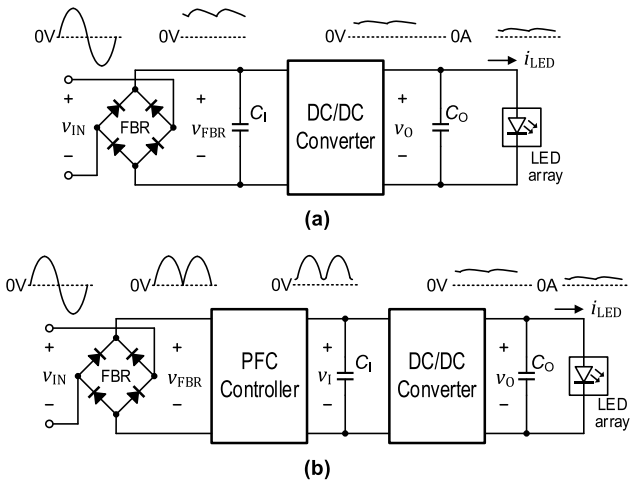

FIGURE 3. Conventional AC/DC conversion topologies. (a) A single-stage conversion and (b) a two-stage conversion.

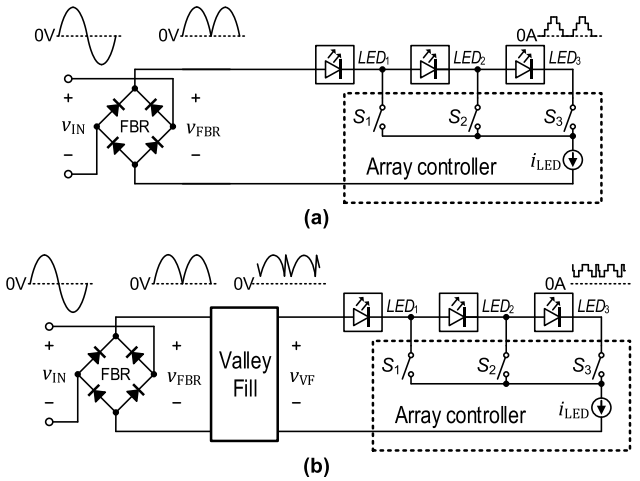

FIGURE 4. Conventional direct AC LED drivers (a) with FBR and LED arrays and (b) with an additional valley fill circuit.

In order to eliminate the bulky inductive components and reduce form factor, direct AC LED drivers in Fig. 4(a) have been researched. The rectified AC input voltage v_{FBR} is directly applied to the LED arrays. According to input voltage value, each LED array is determined on or off by the array controller that can be composed of a control logic, switches, and a current regulator and be implemented by a dedicated IC, a micro-controller, or discrete components.

The current drawn from v_{FBR} is directed only to the LED array LED_1 when the switch S_1 turns on. In sequence, when v_{FBR} reaches a voltage enough to turn on both S_1 and S_2, the LED string current i_{LED} is directed to LED_1 and LED_2. In this way, each switch can be determined when to be turn on, and the current through the LED arrays can be adjusted to a predefined value for each step. However, there a several drawbacks of this topology. First, the average current of each LED array significantly varies, which causes luminance non-uniformity in terms of location. Second, the percent flicker becomes 100% due to no current flown through any LED array for a certain time period.

To alleviate these problems, a direct AC LED driver with a valley fill circuit in Fig. 4(b) have been researched [33]. A valley fill circuit is added to a conventional direct AC LED driver. v_{FBR} under a specified level is boosted by the valley fill circuit, which makes i_{LED} continuously flow through the LEDs to enhance percent flicker. Nonetheless, the percent flicker achieved is only 28% and the non-uniformity due to current imbalance among LED arrays cannot be avoided.

III. PROPOSED FLICKER REDUCTION TECHNIQUE

A. CHARGING PHASE OF AN LED ARRAY

Fig. 5(a) shows a simplified block diagram of the proposed direct AC LED driver with an LED array in parallel with an energy storing capacitor C. When v_{FBR} is higher than the voltage across the LED array, v_{LED}, the input current flows through the LED array and charges the capacitor simultaneously as depicted in Fig. 5(b). In the capacitor point of view, this time period can be noted as the charging phase. Once the string current I_{Str} is regulated to a specific value, the currents through the LED array, i_{LED}, and the capacitor, i_C, satisfy

$$i_{LED}(t) + i_C(t) = I_{Str}. \tag{1}$$

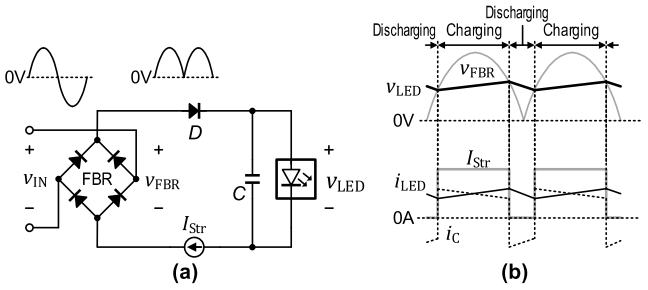

FIGURE 5. Proposed direct AC LED drivers with an always-on LED array. (a) A simplified block diagram and (b) a timing diagram.

Assuming that the LED array consists of m number of LEDs with an ideality factor η and the saturation current I_S, Eq. (1) according to time becomes

$$I_S \exp\left(\frac{v_{LED}(t)}{m\eta V_T}\right) + C\frac{dv_{LED}(t)}{dt} = I_{Str}, \tag{2}$$

where $v_{LED}(t)$ is the voltage across the LED array in terms of time. Then solving the first-order nonlinear ordinary differential equation yields $v_{LED}(t)$ as

$$v_{LED}(t) = -m\eta V_T \cdot \ln\left[\frac{I_S}{I_{Str}} - \frac{1}{I_{Str}}\exp\left\{\frac{c_0 I_{Str}}{m\eta V_T} - \frac{I_{Str}t}{m\eta C V_T}\right\}\right]. \tag{3}$$

If I_S/I_{Str} is a small value, it can be approximated as

$$v_{LED}(t) \approx \frac{I_{Str}}{C}t + c_1, \tag{4}$$

where c_0 and c_1 are constants. c_1 can be obtained as it meets $v_{LED}(0) = V_0$ for initial condition $t = 0$, which gives

$$v_{LED}(t) = \frac{I_{Str}}{C}t + V_0. \tag{5}$$

For the time $t = t_B$ when v_{FBR} goes lower than v_{LED}, the boundary condition yields

$$v_{LED}(t_B) = \frac{I_{Str}}{C}t_B + V_0. \tag{6}$$

From Eq. (5), the LED current equation can be obtained as

$$i_{LED}(t) = I_S \exp\left(\frac{I_{Str}t + V_0 C}{m\eta C V_T}\right). \tag{7}$$

By using the linear approximation of the exponential function for small t values, $f(t) = e^t$ can be approximated as $f(t) \approx 1+t$. Thus $i_{LED}(t)$ can be rewritten as

$$i_{LED}(t) \approx I_S \exp\left(\frac{V_0}{m\eta V_T}\right)\left(1 + \frac{I_{Str}t}{m\eta C V_T}\right). \tag{8}$$

B. DISCHARGING PHASE OF AN LED ARRAY

When the case that v_{FBR} is lower than v_{LED}, on the other hand, the diode D blocks the reverse current flowing from the capacitor to the input and makes the string current be zero. Then the capacitor discharges through the LED array and makes the LED array always on. Eq. (1) can be rewritten as

$$i_{LED}(t) + i_C(t) = 0. \tag{9}$$

Putting the current equations gives

$$I_S \exp\left(\frac{v_{LED}(t)}{m\eta V_T}\right) + C\frac{dv_{LED}(t)}{dt} = 0. \tag{10}$$

Solving the first-order nonlinear differential equation yields $v_{LED}(t)$ as

$$v_{LED}(t) = -m\eta V_T \cdot \left[\ln\left(\frac{I_{Str}}{C}t + c_2\right) - \ln(m\eta V_T)\right], \tag{11}$$

where c_2 is a constant. If the discharging phase is followed by a charging phase, the initial condition of the discharging phase in Eq. (11) at $t = 0$ is identical to the boundary condition of the charging phase in Eq. (6) at $t = t_B$, c_2 can be obtained as

$$c_2 = m\eta V_T \cdot \exp\left[-\frac{1}{m\eta V_T}\left(\frac{I_{Str}}{C}t_B + V_0\right)\right]. \tag{12}$$

Finally, putting Eq. (11) into the LED current equation gives

$$i_{\mathrm{LED}}(t) = I_{\mathrm{S}} \exp\left(\frac{v_{\mathrm{LED}}(t)}{m\eta V_T}\right)$$
$$= I_{\mathrm{S}} \exp\left[\ln(m\eta V_{\mathrm{T}}) - \ln\left(\frac{I_{\mathrm{S}}}{C}t + c_2\right)\right]$$
$$= \frac{m\eta c_2 C V_{\mathrm{T}} I_{\mathrm{S}}}{I_{\mathrm{S}}t + c_2 C}. \quad (13)$$

Assuming that luminance of an LED array is linear to the current through it, percent flicker can be obtained either Eq. (7) or Eq. (13). Using Eq. (7)

$$\%\mathrm{flicker} = \frac{i_{LED}(t_{\mathrm{B}}) - i_{LED}(0)}{i_{LED}(t_{\mathrm{B}}) + i_{LED}(0)}$$
$$= \frac{I_{\mathrm{Str}} t_B}{2m\eta C V_{\mathrm{T}} + I_{\mathrm{Str}} t_B}. \quad (14)$$

The lager the capacitance, the better the percent flicker is. As the string current and thus the rated power increase, an LED array exhibits degradation in the percent flicker. However, the current through a single LED string needs to be regulated in order to meet percent flicker requirement by using a current regulator. The excess voltage other than the regulating the LED string current is applied across the current regulator, which becomes power loss in the current regulator. Thus, having multiple LED arrays and changing the connection among LED arrays depending on the input voltage reduce the excess voltage across the current regulator and thus power loss [29], [30].

C. ANALYSIS OF THE PROPOSED LED ARRAYS

Fig. 6(a) shows the block diagram of the proposed direct AC discrete LED driver with a flicker reduction technique. The proposed LED driver consists of a full bridge rectifier, three LED arrays, a current regulator, a phase-cut/DC converter, and a switch controller. To reduce percent flicker, it is important to make each LED array always turns on. For its implementation, each LED string LED_{1-3} is composed of several LEDs connected in series and connected to each energy storing capacitor C_{1-3} in parallel, respectively. Switches S_{1-3} are implemented by using PNP Darlington pairs and controlled by the signals SC_{1-3}. Once a switch is on, the dedicated LED array is disconnected from the input and fed by its own capacitor that falls into discharge state as discussed in Fig. 5. Each diode D_{1-3} allows each capacitor to be discharged only through the dedicated LED array by floating at least one of the terminals of a capacitor and its LED array. The phase-cut/DC converter generates the reference voltage V_{Ref} to the current regulator that controls the string current as $I_{\mathrm{Str}} = V_{\mathrm{Ref}}/R_{\mathrm{CR}}$ depending on the amount of phase-cut by a TRIAC dimmer.

Depending on switch controls, there can be five different phases as follows: In phase I, all LED arrays are floated from the input and fall into discharging phase. In phases II, III, and IV, only one of LED arrays is floated from the input. In phase V, all the LED arrays are connected to the input. Fig. 6(b) depicts the connection of LED arrays in each phase, when $\mathrm{v}_{\mathrm{LED1}} > \mathrm{v}_{\mathrm{LED2}} > \mathrm{v}_{\mathrm{LED3}}$. The gray colored LED array

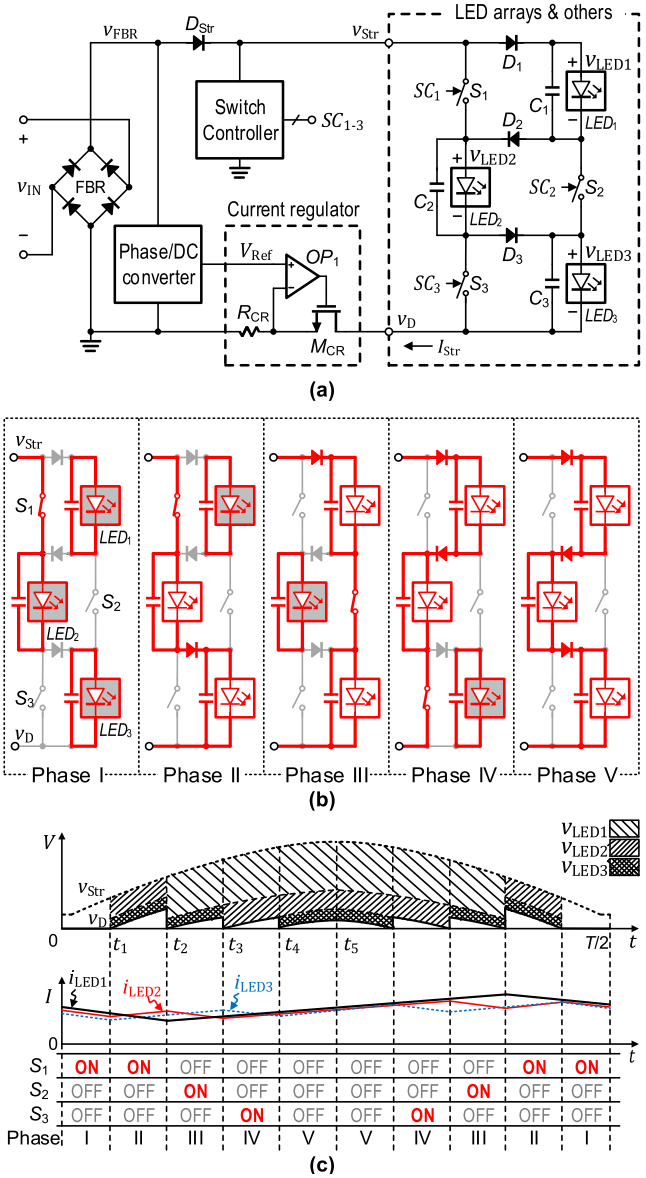

FIGURE 6. The proposed direct AC LED driver. (a) Block diagram, (b) the current through the LED array for each phase, and (c) timing diagram.

indicates the LED array powered by its dedicated capacitor. Regardless of configuration, all LED arrays are continuously powered either from the input or from their own capacitors, which allows for low percent flicker in the proposed direct AC LED driver. Fig. 6(c) shows the voltage and the current waveforms of each LED array for the half cycle of v_{IN}. The sequence of switching of the proposed LED driver is chosen to increase the efficiency by minimizing energy loss by the current regulator, $\mathrm{E}_{\mathrm{LossCR}}$, as follows:

1) Phase I: If $\mathrm{v}_{\mathrm{Str}} < \mathrm{v}_{\mathrm{LED2}} + \mathrm{v}_{\mathrm{LED3}}$, S_1 turns on, while S_2 and S_3 turn off. Then all LED arrays are floated and fed the current from each dedicated capacitor.
2) Phase II: If $\mathrm{v}_{\mathrm{LED2}} + \mathrm{v}_{\mathrm{LED3}} < \mathrm{v}_{\mathrm{Str}} < \mathrm{v}_{\mathrm{LED1}} + \mathrm{v}_{\mathrm{LED3}}$, S_1 turns on, while S_2 and S_3 turn off. Then $\mathrm{I}_{\mathrm{Str}}$ flows through LED_2 and LED_3 and charges their dedicated

capacitors C_2 and C_3. The current through LED_1 is fed by C_1.

3) Phase III: If $v_{LED1}+v_{LED3} < v_{Str} < v_{LED1}+v_{LED2}$, S_2 turns on, while S_1 and S_3 turn off. Then I_{Str} flows only through LED_1 and LED_3 and charges their dedicated capacitors C_1 and C_3. The current through LED_2 is fed by C_2.
4) Phase IV: If $v_{LED1}+v_{LED2} < v_{Str} < v_{LED1}+v_{LED2}+v_{LED3}$, S_3 turns on, while S_1 and S_2 turn off. Then I_{Str} flows only through LED_1 and LED_2 and charges their dedicated capacitors C_1 and C_2. The current through LED_3 is fed by C_3.
5) Phase V: If $v_{LED1}+v_{LED2}+v_{LED3} < v_{Str}$, all switches turn off. Then I_{Str} flows through the strings LED_1, LED_2, and LED_3 and charges all capacitors C_1, C_2, and C_3.

D. OPTIMUM CONFIGURATION OF LEDS

Because I_{Str} is regulated by the current regulator, the power from the input can be defined as

$$P_{IN}(t) = I_{Str} V_P \sin(2\pi ft), \tag{15}$$

where V_P is the peak value of the sinusoidal input voltage. Using quarter-wave symmetry, the energy input in a cycle can be written as

$$E_{IN} = 4I_{Str} \int_o^{T/4} V_P \sin(2\pi ft) dt. \tag{16}$$

In phase I, the string current becomes zero due to the input floated from any of the LED array. Then the average input power can be

$$\langle P_{IN} \rangle = \frac{4I_{Str}}{T} \int_{t_1}^{T/4} V_P \sin(2\pi ft) dt, \tag{17}$$

where t_1 is defined as the time when the phase I ends and can be a constant for a given input power as

$$t_1 = \frac{1}{2\pi f} \cos^{-1}\left(\frac{\pi \langle P_{IN} \rangle}{2I_{Str} V_P}\right). \tag{18}$$

Assuming that the current ripple is much smaller than its average value, the efficiency of the proposed system, η, can be optimized by maximizing the sum of shaded area from A_2 to A_5 in Fig. 7 as

$$\langle P_O \rangle \propto \int_{t_1}^{T/4} (v_{Str}(t) - v_D(t)) dt. \tag{19}$$

Defining that each array has a certain number of LEDs in series and the average values of the voltage across each LED array are m_1 $<v_{LED}>$, m_2 $<v_{LED}>$, and m_3 $<v_{LED}>$ where $<v_{LED}>$ stands for the average voltage across an LED, the relationship among each LED array can be $m_1 > m_2 > m_3$. Then, each shaded area can be defined as

$$A_2 = (m_2 + m_3)(t_2 - t_1) \langle v_{LED} \rangle, \tag{20}$$
$$A_3 = (m_1 + m_3)(t_3 - t_2) \langle v_{LED} \rangle, \tag{21}$$
$$A_4 = (m_1 + m_2)(t_4 - t_3) \langle v_{LED} \rangle, \tag{22}$$

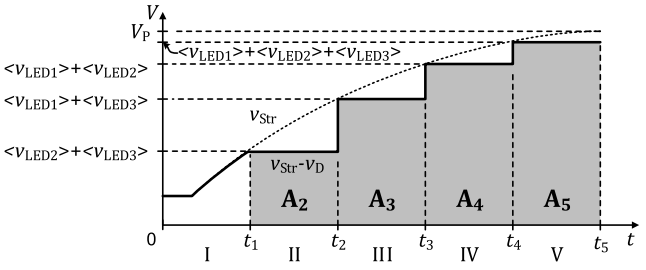

FIGURE 7. Maximizing the conversion efficiency of the proposed LED arrays.

$$A_5 = (m_1 + m_2 + m_3)(t_5 - t_4) \langle v_{LED} \rangle. \tag{23}$$

Then the sum of the shaded area becomes

$$\sum_i A_i = \langle v_{LED} \rangle [(m_2 + m_3)(t_2 - t_1) + (m_1 + m_3)(t_3 - t_2) + (m_1 + m_2)(t_4 - t_3) + (m_1 + m_2 + m_3)(t_5 - t_4)], \tag{24}$$

where t_5 is T/4. t_1, t_2, t_3, and t_4 can be obtained at each edge of phase from $v_{Str} = V_P \sin(2\pi$ ft) as

$$t_2 = \sin^{-1}((m_1 + m_3) \langle v_{LED} \rangle / V_P) / (2\pi f), \tag{25}$$
$$t_3 = \sin^{-1}((m_1 + m_2) \langle v_{LED} \rangle / V_P) / (2\pi f), \tag{26}$$
$$t_4 = \sin^{-1}((m_1 + m_2 + m_3) \langle v_{LED} \rangle / V_P) / (2\pi f). \tag{27}$$

In determining each timing, the basic condition is

$$V_P > (m_1 + m_2 + m_3) \langle v_{LED} \rangle. \tag{28}$$

E. SWITCH CONTROLLER

Fig. 8(a) shows the circuit diagram of the switch controller. A voltage divider is located in the dotted box, which generates the switch control voltages v_{1-3} out of v_{Str}. A Zener diode D_{Z1} and a capacitor C_{Z1} generate a bias voltage V_B to control the outputs SC_{1-3} through bipolar junction transistors Q_{1-3}. Depending on the values of v_{1-3}, the base terminals of Q_{1-3} can be grounded through M_{1-3} and Q_{4-6}. SC_{1-3} are fed to the base currents of PNP Darlington pair switches S_{1-3}, respectively. The operation of each transistor depending on v_{1-3} and phase is depicted in Fig. 8(b).

F. PHASE-CUT/DC CONVERTER

Fig. 9(a) shows the circuit diagram of the phase-cut/DC converter. When v_{FBR} is higher than the Zener voltage V_Z of D_{Z2}, the gate voltage of M_4, v_G, equals to V_Z. Otherwise, v_G remains to be v_{FBR}. Then, v_S is defined by the resistive voltage divider as

$$v_S = (v_G - V_{Th}) \cdot \frac{R_8}{R_7 + R_8}, \tag{29}$$

where V_{Th} is the threshold voltage of M_4. v_S is connected to a passive RC low-pass filter and generates the reference voltage V_{Ref} that depends on the phase-cut ratio. The voltage waveforms of each node without phase-cut and with 50% phase-cut are depicted in Figs. 9(b) and 9(c).

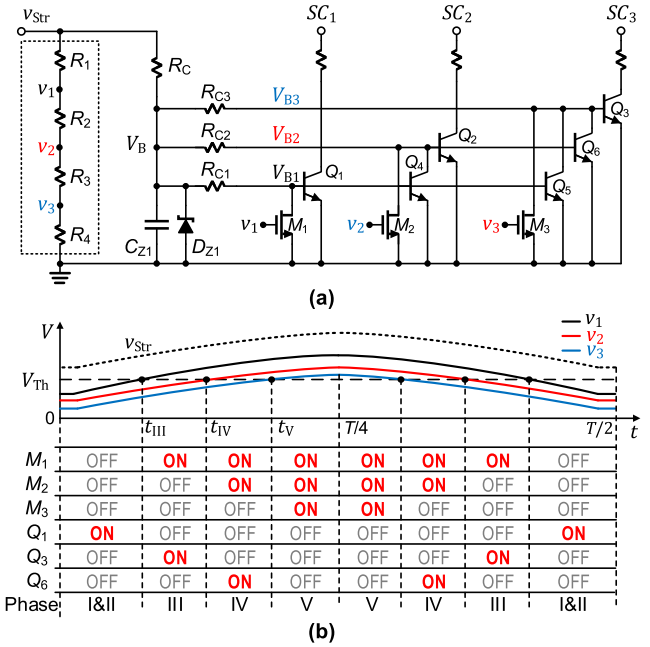

FIGURE 8. Proposed switch controller. (a) Circuit and (b) timing diagrams.

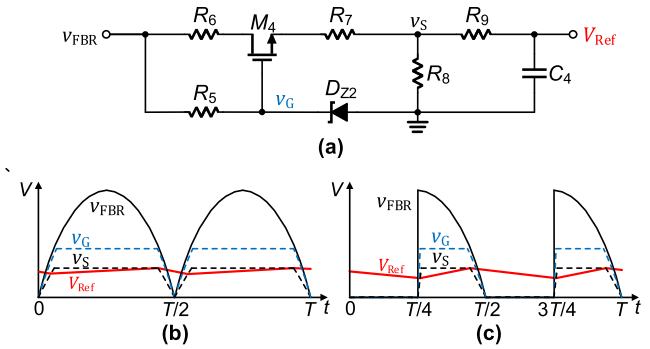

FIGURE 9. Proposed phase-cut/DC converter. (a) Circuit implementation and (b) timing diagrams without phase-cut and (c) with 40% phase-cut.

IV. SIMULATION RESULTS

Fig.10 shows the simulation results in determining the number of LED strings of the proposed LED driver.

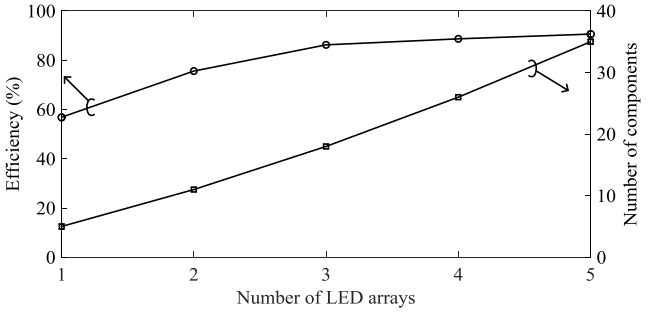

FIGURE 10. Simulated results for efficiency and the number of components according to the number of LED arrays.

Efficiency and the number of critical components including capacitors, diodes, and switches are depending on the number of LED arrays. The more the LED arrays, the higher the efficiency is achieved. The proposed driver is chosen to have three LED arrays because the efficiency enhancement is only 4.4% at the expense of 1.94 times more components compared to the configuration with five LED arrays. For maximizing the sum of shaded area from $\mathbf{A}_2$ to $\mathbf{A}_5$, $< v_{\mathrm{LED}} >$ and $< P_{\mathrm{IN}} >$ are set to 6 V @ 110 mA and 15 W. By sweeping m_1 and m_2 with various integer values of m_3, the sum of the shaded area that meets the condition in Eq. (18) is depicted in Fig. 11. The differences between the maximum area and the area with quantized values of m_1 and m_2 are less than 1%. The maximum area with integer values of m_1, m_2, and m_3 is given by 20.88 Vs @ ($m_1 = 12$, $m_2 = 8$, $m_3 = 4$). The proposed LED driver is also simulated by using SPICE parameters.

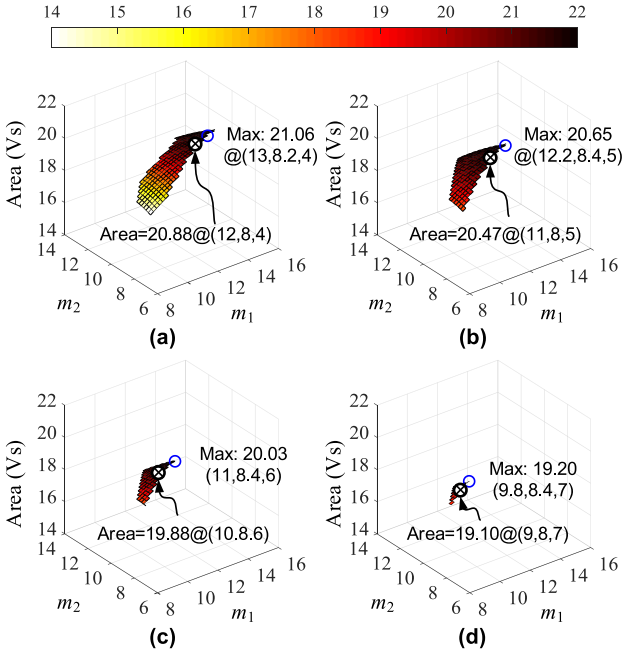

FIGURE 11. Simulated results for Maximizing the sum of Area $\mathbf{A}_{2-5}$ (a) $m_3 = 4$, (b) $m_3 = 5$, (c) $m_3 = 6$, and (d) $m_3 = 7$.

Fig. 12 shows the simulated transient waveforms of the proposed direct AC LED driver without phase-cut. Both the input current and the current through the LED arrays LED_{1-3} are depicted. Since the LED current can be approximated as linear to the luminous flux output of the LED, percent flicker can be calculated by using the LED current. The simulated percent flicker of each LED string LED_1, LED_2, and LED_3 are 18.6, 18.5, and 17.9%, respectively, and the simulated percent flicker of overall LEDs is 18.3%. Fig. 13 shows the transient waveform of the switch controller.

$\mathrm{V}_{\mathrm{B1-3}}$ in Fig. 8 are turned on and off sequentially depending on v_{1-3}. Fig. 14 shows the transient waveforms of the phase-cut/DC converter to obtain $\mathrm{V}_{\mathrm{Ref}}$, where the settling time of $\mathrm{V}_{\mathrm{Ref}}$ is 0.05 s with no phase-cut. $\mathrm{V}_{\mathrm{Ref}}$ according to various values of the phase-cut ratio is presented in Fig.15,

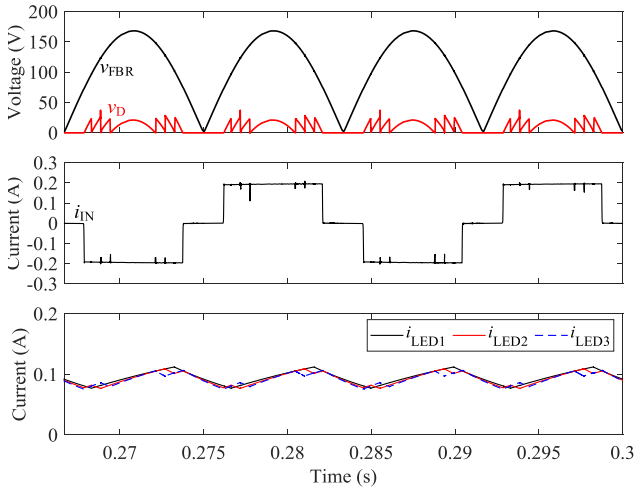

FIGURE 12. Simulated transient waveforms of the proposed direct AC LED driver without phase-cut.

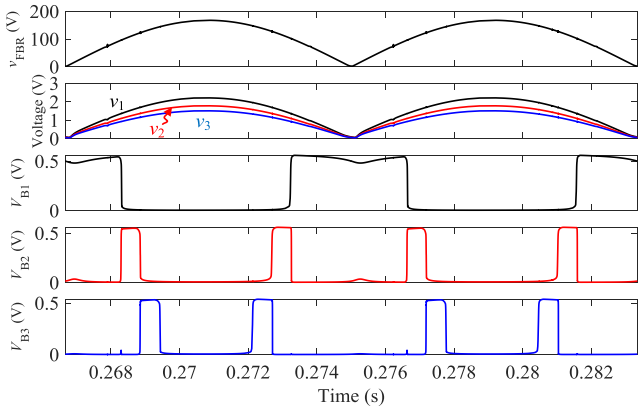

FIGURE 13. Simulated transient waveforms of the switch controller.

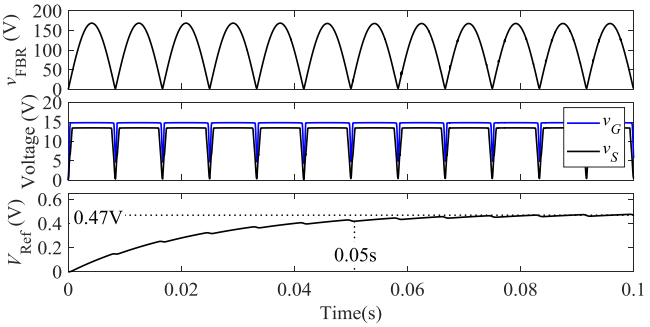

FIGURE 14. Simulated transient waveforms of the proposed direct AC LED driver without phase-cut.

which leads V_{Ref} inversely proportional to the phase-cut ratio. As V_{Ref} decreases, so do I_{Str} and the luminance of each LED array.

V. EXPERIMENTAL RESULTS

The proposed LED driver is implemented only with discrete components. Fig. 16 shows the photograph of the proposed LED lighting. The diameter of the metal PCB is 100 mm.

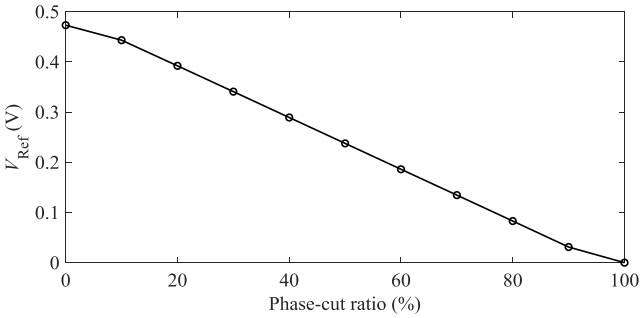

FIGURE 15. Simulated reference value V_{Ref} according to the phase-cut ratio of the phase-cut/DC converter.

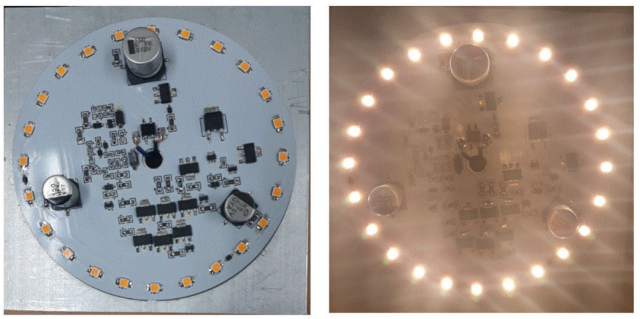

FIGURE 16. Photograph of the proposed LED driver.

The number of LEDs in LED_{1-3} is 12, 8, and 4, respectively. C_{1-3} are set to 150, 150, and 270 μF with the rated voltage of 80, 50, and 35 V, respectively. The critical components of the proposed driver are listed in Table 1.

TABLE 1. Critical components of the proposed LED driver.

Component	Description
Rectifier	Full bridge, 200V, 1A
D_{Str}	String diode, 200V, 1A
D_1-D_3	Switching diode, 100V, 0.5A
S_1-S_3	PNP Darlington switch, 120V, 2A
Q_1-Q_6	NPN, 180V, 0.5A
M_1-M_3	NMOS, 100V, 0.17A
LED_{1-3}	LEDs, LEMWS36X80LZ3B00
C_1	150 µF, 80 V, electrolytic
C_2	150 µF, 50 V, electrolytic
C_3	270 µF, 35 V, electrolytic
OP_1	Op-amp, MCP6281

Nominal output power is 15W for the input voltage ranging from 80 to 140V. The average value of V_D is minimized for each phase to enhance the efficiency of the proposed LED driver as simulated in Fig. 11, which leads to the measured efficiency of 84.7%.

Fig. 17(a) shows the measured transient waveforms of v_{FBR}, v_D and i_{IN} with the phase-cut ratio of 0%. The power factor extracted from i_{IN} yields 96.8% at 120 V input. To obtain percent flicker as in [38], the brightness of the LED arrays for the proposed LED driver is measured with a light-to-voltage optical sensor TSL251RD as

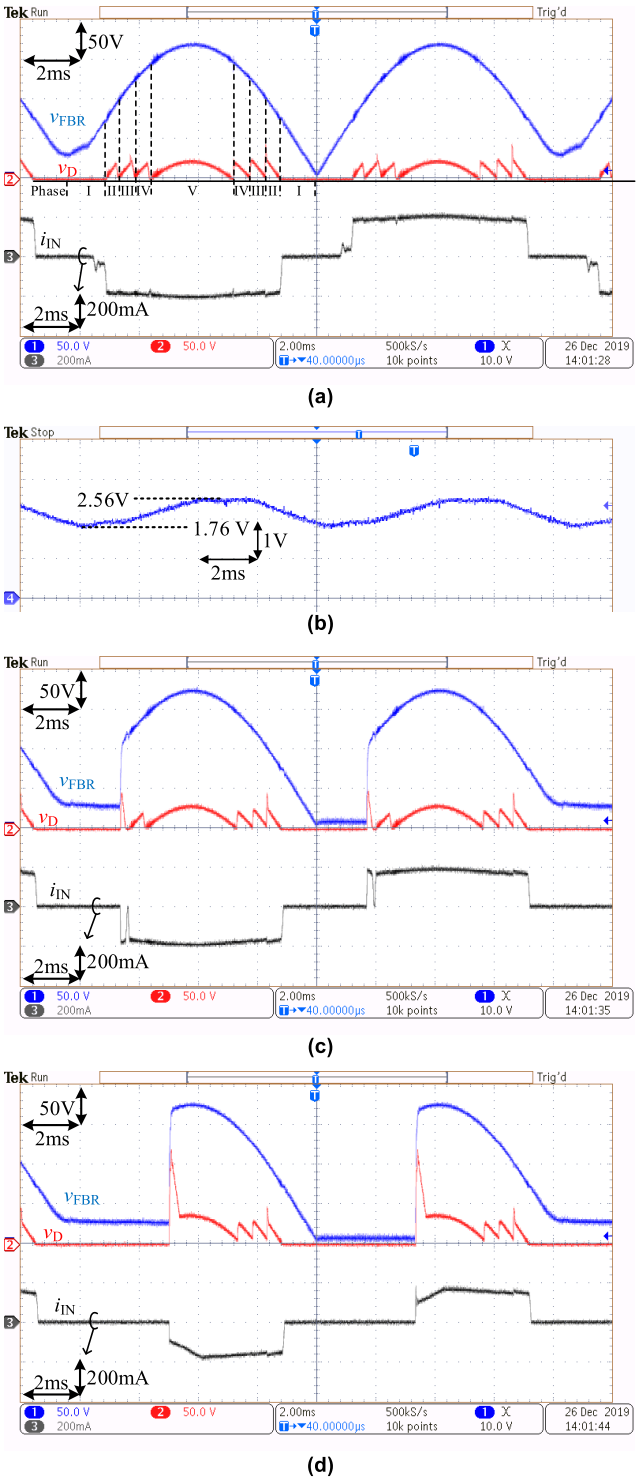

FIGURE 17. Measured transient response of the proposed LED driver with (a) 0%, (b) Measured brightness of LEDs (c) 20%, and (d) 40% phase-cut.

shown in Fig. 17(b). The measured percent flicker obtained as 18.6%. Figs. 17(c) and 17(d) show the measured transient waveforms v_{FBR}, v_D, and i_{IN} with the phase-cut ratio of 20 and 40%. At the phase-cut angle, glitches caused by RC delay in V_{B1}, V_{B2}, and V_{B3} turn on switches S_1, S_2, and S_3 momentarily, make v_D to be v_{FBR}, and cause sharp rise

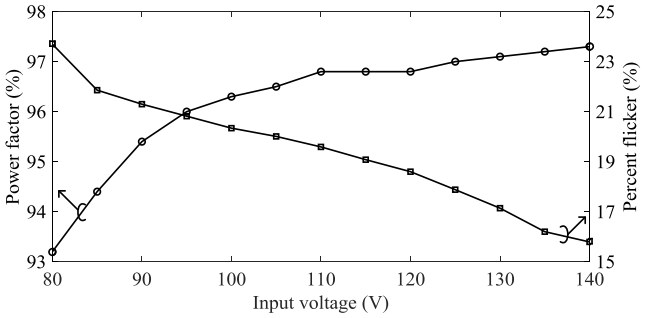

FIGURE 18. Measured power factor and percent flicker according to the input voltage.

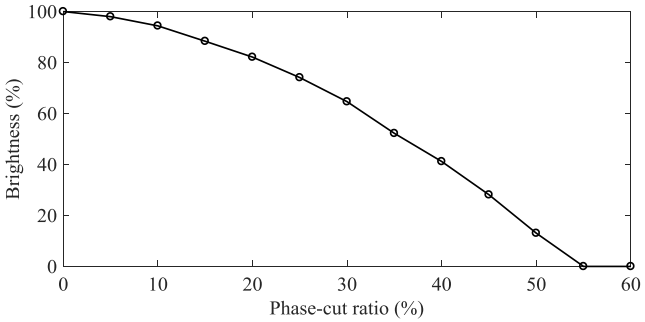

FIGURE 19. Measured average brightness according to the phase-cut ratio.

in v_D. Thus, a high voltage transistor is required for M_{CR} in Fig. 6(a). By sweeping the input voltage ranged from 80 to 140 V at phase-cut ratio 0%, power factor and percent flicker are measured as shown in Fig. 18. The power factor and the percent flicker of the proposed driver at the input voltage range from 80 to 140 V are achieved at the range from 93.2% to 97.3% and from 15.79% to 23.7%, respectively. Fig. 19 summarizes measured average brightness according to the phase-cut ratio at 120V input. For phase-cut ratio higher than 55.6%, the proposed direct AC LED driver turns off completely. The proposed LED driver is compared with other conventional direct AC LED drivers as shown in Table 2.

TABLE 2. Performance comparison.

Parameter	[30]	[31]	[32]	[33]	[34]	**This work**
Dedicated-IC free	X	O	O	O	O	**O**
TRIAC dimmable	X	X	X	X	X	**O**
Always-on	X	X	X	X	X	**O**
$V_{IN(AC)}$ (V)	110	85~265	42.4	220	110	**80-140**
P_{OUT} (W)	19	20	2.5	N/A	3.6	**15**
Power factor (%)	99.8	>90	97	99	72	**97.3**
Percent flicker (%)	100	100	100	100	28	**18.6**
Efficiency (%)	89.3	92.4	82	N/A	N/A	**84.7**

"X" stands for not applicable and "O" stands for applicable

The proposed LED driver is superior to other direct AC LED drivers not only percent flicker but also TRIAC compatibility and always-on capability that increases uniformity

among LED arrays. Moreover, no dedicated IC or controller is required for supporting compatible performances with others.

VI. CONCLUSION

In order to replace conventional lamps with LEDs, nowadays, LED drivers are required to meet IEEE PAR1789 standard to reduce health risks by higher percent flicker. Moreover, LED driver compatible to a TRIAC dimmer can be widely used for various applications. The proposed direct AC LED driver supports above two characteristics without using a dedicated IC, which no conventional direct AC LED driver has ever achieved. Other performances achieved by the proposed direct AC LED driver such as efficiency and power factors are comparable to others.

REFERENCES

[1] J. Y. Tsao, "Solid-state lighting: Lamps, chips, and materials for tomorrow," *IEEE Circuits Devices Mag.*, vol. 20, no. 3, pp. 28–37, May 2004.

[2] I. L. Azevedo, M. G. Morgan, and F. Morgan, "The transition to solid-state lighting," *Proc. IEEE*, vol. 97, no. 3, pp. 481–510, Mar. 2009.

[3] S. Moon, G.-B. Koo, and G.-W. Moon, "Dimming-feedback control method for TRIAC dimmable LED drivers," *IEEE Trans. Ind. Electron.*, vol. 62, no. 2, pp. 960–965, Feb. 2015.

[4] C. Ye, P. Das, and S. Kumar Sahoo, "Peak current control of multichannel LED driver with selective dimming," *IEEE Trans. Ind. Electron.*, vol. 66, no. 5, pp. 3446–3457, May 2019.

[5] P. Liu, Z. Hong, and C. Hung, "A single-stage low-power AC-DC RGB-LED driver with switching capacitor control scheme," *IEEE Trans. Ind. Electron*, early access, Mar. 11, 2020, doi: 10.1109/TIE.2020.2978705.

[6] D. Rand, B. Lehman, and A. Shteynberg, "Issues, models and solutions for triac modulated phase dimming of LED lamps," in *Proc. IEEE Power Electron. Spec. Conf.*, Oct. 2007, pp. 1398–1404.

[7] *IEEE Recommended Practices for Modulating Current in High-Brightness LEDs for Mitigating Health Risks to Viewers*, IEEE Standard 1789-2015, 2015. [Online]. Available: https://standards.ieee.org/standard/1789-2015.html

[8] B. Lehman and A. J. Wilkins, "Designing to mitigate effects of flicker in LED lighting: Reducing risks to health and safety," *IEEE Power Electron. Mag.*, vol. 1, no. 3, pp. 18–26, Sep. 2014.

[9] W. Chen and S. Y. R. Hui, "Elimination of an electrolytic capacitor in AC/DC light-emitting diode (LED) driver with high input power factor and constant output current," *IEEE Trans. Power Electron.*, vol. 27, no. 3, pp. 1598–1607, Mar. 2012.

[10] R. Zhang and H. S.-H. Chung, "A TRIAC-dimmable LED lamp driver with wide dimming range," *IEEE Trans. Power Electron.*, vol. 29, no. 3, pp. 1434–1446, Mar. 2014.

[11] Y. Wang, Y. Guan, D. Xu, and W. Wang, "A CLCL resonant DC/DC converter for two-stage LED driver system," *IEEE Trans. Ind. Electron.*, vol. 63, no. 5, pp. 2883–2891, May 2016.

[12] J. Zhang, T. Jiang, and X. Wu, "A high-efficiency quasi-two-stage LED driver with multichannel outputs," *IEEE Trans. Ind. Electron.*, vol. 64, no. 7, pp. 5875–5882, Jul. 2017.

[13] C. Ye, P. Das, and S. K. Sahoo, "Peak current control-based power ripple decoupling of AC–DC multichannel LED driver," *IEEE Trans. Ind. Electron.*, vol. 66, no. 12, pp. 9248–9259, Dec. 2019.

[14] D. Gacio, J. M. Alonso, A. J. Calleja, J. Garcia, and M. Rico-Secades, "A universal-input single-stage high-power-factor power supply for HB-LEDs based on integrated buck-flyback converter," *IEEE Trans. Ind. Electron.*, vol. 58, no. 2, pp. 589–599, Feb. 2011.

[15] D. G. Lamar, M. Fernandez, M. Arias, M. M. Hernando, and J. Sebastian, "Tapped-inductor buck HB-LED AC–DC driver operating in boundary conduction mode for replacing incandescent bulb lamps," *IEEE Trans. Power Electron.*, vol. 27, no. 10, pp. 4329–4337, Oct. 2012.

[16] Y. Hu, L. Huber, and M. M. Jovanović, "Single-stage, universal-input AC/DC LED driver with current-controlled variable PFC boost inductor," *IEEE Trans. Power Electron.*, vol. 27, no. 3, pp. 1579–1588, Mar. 2012.

[17] X. Wu, J. Yang, J. Zhang, and Z. Qian, "Variable on-time (VOT)-controlled critical conduction mode buck PFC converter for high-input AC/DC HB-LED lighting applications," *IEEE Trans. Power Electron.*, vol. 27, no. 11, pp. 4530–4539, Nov. 2012.

[18] Y.-C. Li and C.-L. Chen, "A novel single-stage high-power-factor AC-to-DC LED driving circuit with leakage inductance energy recycling," *IEEE Trans. Ind. Electron.*, vol. 59, no. 2, pp. 793–802, Feb. 2012.

[19] Y.-C. Li and C.-L. Chen, "A novel primary-side regulation scheme for single-stage high-power-factor AC–DC LED driving circuit," *IEEE Trans. Ind. Electron.*, vol. 60, no. 11, pp. 4978–4986, Nov. 2013.

[20] B. Poorali and E. Adib, "Analysis of the integrated SEPIC-flyback converter as a single-stage single-switch power-factor-correction LED driver," *IEEE Trans. Ind. Electron.*, vol. 63, no. 6, pp. 3562–3570, Jun. 2016.

[21] P.-J. Liu and K.-L. Peng, "Adaptive driving bus voltage and energy recycling control schemes for low-power AC–DC RGB-LED drivers," *IEEE Trans. Ind. Electron.*, vol. 64, no. 10, pp. 7741–7748, Oct. 2017.

[22] P. Fang, S. Webb, Y. Chen, Y.-F. Liu, and P. C. Sen, "A multiplexing ripple cancellation LED driver with true single-stage power conversion and flicker-free operation," *IEEE Trans. Power Electron.*, vol. 34, no. 10, pp. 10105–10120, Oct. 2019.

[23] M. Kadota, H. Shoji, H. Hirose, A. Hatakeyama, and K. Wada, "A turn-off delay controlled bleeder circuit for single-stage TRIAC dimmable LED driver with small-scale implementation and low output current ripple," *IEEE Trans. Power Electron.*, vol. 34, no. 10, pp. 10069–10081, Oct. 2019.

[24] Y. Wang, F. Li, Y. Qiu, S. Gao, Y. Guan, and D. Xu, "A single-stage LED driver based on flyback and modified Class-E resonant converters with low-voltage stress," *IEEE Trans. Ind. Electron.*, vol. 66, no. 11, pp. 8463–8473, Nov. 2019.

[25] *Datasheet: DN05079/D Direct-AC, Linear LED Driver Topology by ON Semiconductor, Rev. 0*, Aug. 2015.

[26] Texas Instruments, Dallas, TX, USA. *TPS92411x Floating Switch for Ofine AC Linear Direct Drive of LEDs With Low Ripple Current (Revision B)*. Accessed: Nov. 2, 2020. [Online]. Available: http://www.ti.com/Product/TPS92411

[27] S. Y. Hui, S. N. Li, X. H. Tao, W. Chen, and W. M. Ng, "A novel passive offline LED driver with long lifetime," *IEEE Trans. Power Electron.*, vol. 25, no. 10, pp. 2665–2672, Oct. 2010.

[28] C. Park and C.-T. Rim, "Filter-free AC direct LED driver with unity power factor and low input current THD using binary segmented switched LED strings and linear current regulator," in *Proc. 28th Annu. IEEE Appl. Power Electron. Conf. Expo. (APEC)*, Mar. 2013, pp. 870–874.

[29] D. Gu, S. Tang, J. Xi, L. He, and K. Sun, "A dimmable and power-compensated AC direct LED driver with high efficiency," in *Proc. IEEE Int. SoC Design Conf.*, Oct. 2016, pp. 343–344.

[30] N. Ning, C. B. Wang, C. Y. Feng, D. J. Yu, and W. B. Chen, "Self-adaptive load technology for multiple-string LED drivers," *Electron. Lett.*, vol. 49, no. 18, pp. 1170–1171, Aug. 2013.

[31] Y.-C. Chung, K.-M. Lee, H.-J. Choe, C.-H. Sung, and B. Kang, "Low-cost drive circuit for AC-direct LED lamps," *IEEE Trans. Power Electron.*, vol. 30, no. 10, pp. 5776–5782, Oct. 2015.

[32] R. Dayal, K. Modepalli, and L. Parsa, "A direct AC LED driver with high power factor without the use of passive components," in *Proc. IEEE Energy Convers. Congr. Expo. (ECCE)*, Sep. 2012, pp. 4230–4234.

[33] J. Fu, G. Wang, S. Wang, Z. Chen, and L. Shi, "A novel AC direct linear LED driver with unity power factor, low input current THD, low light flicker and low profile," in *Proc. PCIM Eur., Int. Exhib. Conf. Power Electron. Intel. Motion, Renew. Energy Energy Manag.*, Jun. 2018, pp. 1–7.

[34] Y. Li, J. Han, and S. Sanders, "A low cost AC direct LED driver with reduced flicker using triac," in *Proc. IEEE Energy Convers. Congr. Expo. (ECCE)*, Sep. 2018, pp. 4738–4743.

[35] J.-E. Park, J.-W. Kim, B.-H. Lee, and G.-W. Moon, "Design on topologies for high efficiency two-stage AC-DC converter," in *Proc. 7th Int. Power Electron. Motion Control Conf.*, Harbin, China, Jun. 2012, pp. 257–262.

[36] M. Wlas and S. Galla, "The influence of LED lighting sources on the nature of power factor," *Energies*, vol. 11, no. 6, pp. 4738–4743, Jun. 2018.

[37] J. He, X. Ruan, and L. Zhang, "Adaptive voltage control for bidirectional converter in flicker-free electrolytic capacitor-less AC–DC LED driver," *IEEE Trans. Ind. Electron.*, vol. 64, no. 1, pp. 320–324, Jan. 2017.
[38] Y. Gao, L. Li, and P. K. T. Mok, "An AC input switching-converter-free LED driver with low-frequency-flicker reduction," *IEEE J. Solid-State Circuits*, vol. 52, no. 5, pp. 1424–1434, May 2017.

SEONG JIN YUN (Member, IEEE) received the B.S. and M.S. degrees in electrical engineering from Kangwon National University (KNU), South Korea, in 2010 and 2012, respectively. He is currently pursuing the Ph.D. degree with Korea University, Seoul, South Korea. From December 2011 to August 2013, he worked as a Research Engineer with Dongbu Hitek Inc., Seoul, designing digital circuits and systems for large display driver IC (LDDI). His research interests include direct ac LED driver for flicker reduction, low dropout (LDO) voltage regulator for system-on-chip (SoC) applications, and power management ICs design. He was a recipient of the 2010 KEC Analog Circuit Design Contest. He also received the IP Design Contest of Dongbu Hitek Inc., in 2011.

YONG KI YUN (Graduate Student Member, IEEE) received the B.S. degree in electrical engineering from Seokyeong University, Seoul, South Korea, in 2019. He is currently pursuing the M.S. degree with Korea University, Seoul. His research interests include direct ac LED driver for flicker reduction and power management ICs.

YONG SIN KIM (Senior Member, IEEE) received the B.S. and M.S. degrees in electronics from Korea University, Seoul, South Korea, in 1999 and 2003, respectively, and the Ph.D. degree in electrical engineering from the University of California at Santa Cruz, USA in 2008. From 2008 to 2012, he worked with the University of California Advanced Solar Technologies Institute (UC Solar), where he researched on optimizing power in distributed photovoltaic systems. From 2012 to 2014, he was with the School of Electrical and Electronics Engineering, Chung-Ang University, Seoul, where he was involved in development of sensors for human-machine interface. Since March 2014, he has been with the School of Electrical Engineering, Korea University. His current research interests include cross-disciplinary integration of circuits and systems for energy harvesting and sensor applications.